J|A|C|S
ARTICLES
Published on Web 01/26/2007

Dissecting the Thermodynamics and Cooperativity of Ligand Binding in Cytochrome P450eryF

B. K. Muralidhara,*,† Surendra S. Negi,‡ and James R. Halpert†

Contribution from the Department of Pharmacology and Toxicology, and Sealy Center for Structural Biology, University of Texas Medical Branch, 301 University Boulevard, Galveston, Texas 77555

Received August 30, 2006; E-mail: bkmurali@utmb.edu

Abstract: Conformational flexibility and cooperativity in ligand recognition are two key aspects of the catalytic diversity of cytochrome P450 enzymes. In this study, we dissect the ligand binding stoichiometry and energetics of the soluble bacterial P450eryF by isothermal titration calorimetry (ITC) using three allosteric and two non-allosteric ligands of diverse chemistry. Complementary spectral binding studies and sequential, two-ligand docking simulations were performed to help assign the binding sites. Binding of 4-phenylpyridine (4-PP) or 4-(4-chlorophenyl)imidazole (4-CPI) showed 1:1 stoichiometry in ITC, consistent with the lack of cooperativity observed in spectral binding studies. The larger ligands 9-aminophenanthrene (9-AP), 1-pyrenebutanol (1-PB), and α-naphthoflavone (ANF) show cooperative spectral binding and yielded 2:1 stoichiometry. The associated thermodynamic parameters for the sites were calculated using a sequential binding mechanism. The binding constant (K_D) for the first site was almost two times lower than that of the second site for all three compounds. Ligand binding at site 1 was entropically favored, whereas binding at site 2 was weak and entropically unfavorable. Simulations showed that two molecules of 9-AP, ANF or 1-PB can be adequately docked to two individual sub-sites within a large binding pocket. The absence of hydrophobic tethering and ligand stacking are consistent with the single low affinity binding site observed for 4-CPI and 4-PP. Competitive binding studies with P450eryF preloaded with either 1-PB or ANF showed a decrease in the affinities for 9-AP at both the sites, with large entropy−enthalpy compensation, indicating the ability of the binding pocket to accommodate two ligands of diverse chemistry and enable cooperativity.

Introduction

Cytochromes P450 (P450s) are among the most catalytically diversified protein molecules, with the ability to catalyze selective oxidative reactions on a wide variety of substrates despite a conserved tertiary fold.[1] In addition to broad substrate specificity, the cooperativity in substrate recognition and metabolism exhibited by many mammalian (3A4, 2C9, 1A2, 2D6, and 2B6) and bacterial (P450eryF) P450s is a phenomenon of added complexity that is not well understood. Despite the rapidly increasing knowledge of the three-dimensional structures of mammalian P450s,[2−9] cooperativity remains a challenge in understanding drug−drug interactions and predicting drug incompatibilities. The prevailing hypothesis is that the P450s exhibiting cooperativity bind multiple (at least two) ligands in one large binding pocket, in which a loose fit of the first molecule requires binding of an additional ligand for effective catalysis.[10−15] However, the binding of an effector away from the active site has also been suggested for CYP3A4,[12,16,17] and direct evidence for a distal binding site for progesterone was derived by X-ray crystallography.[8] The persistent conformational heterogeneity related to the oligomeric state of CYP3A4 in solution adds additional complexity to the analysis of cooperativity.[19−21] Recently, our laboratory employed innovative FRET and Job's titration methods to study ligand-dependent allostery

† Department of Pharmacology and Toxicology.
‡ Sealy Center for Structural Biology.

(1) Poulos, T. L.; Johnson, E. F. *Cytochrome P450: Structure, Mechanism and Biochemistry*, 3rd ed.; Ortiz de Montellano, P. R., Ed.; Plenum Publishers: New York, 2005; pp 87−114.
(2) Cupp-Vickery, J.; Anderson, R.; Hatziris, Z. *Proc. Natl. Acad. Sci. U.S.A.* **2000**, *97*, 3050−3055.
(3) de Groot, M. J. *Drug Discovery Today* **2006**, *11*, 601−606.
(4) Scott, E. E.; He, Y. A.; Wester, M. R.; White, M. A.; Chin, C. C.; Halpert, J. R.; Johnson, E. F.; Stout, D. *Proc. Natl. Acad. Sci. U.S.A.* **2003**, *100*, 13196−13201.
(5) Scott, E. E.; White, M. A.; He, Y. A.; Johnson, E. F.; Stout, D.; and Halpert, J. R. *J. Biol. Chem.* **2004**, *279*, 27294−27301.
(6) Wester, M. R.; Yano, J. K.; Schoch, G. A.; Yang, C.; Griffin, K. J.; Stout, C. D.; Johnson, E. F. *J. Biol. Chem.* **2004**, *279*, 35630−35637.
(7) Williams, P. A.; Cosme, J.; Angove, H. C.; Vinkovic, D. M.; Jhoti, H. *Nature* **2003**, *424*, 464−468.
(8) Williams, P. A.; Cosme, J.; Vinkovic, D. M.; Ward, A.; Angove, H. C.; Day. P. J.; Vonrhein, C.; Tickle, I. J.; Jhoti, H. *Science* **2004**, *305*, 683−686.
(9) Zhao, Y.; White, W. A.; Muralidhara, B. K.; Sun, L.; Halpert, J. R.; Stout, C. D. *J. Biol. Chem.* **2006**, *281*, 5973−5981.
(10) Shou, M.; Grogan, J.; Mancewicz, J. A.; Krausz, K. W.; Gonzalez, F. J.; Gelboin, H. V.; Korzekwa, K. R. *Biochemistry* **1994**, *33*, 6450−6455.
(11) Korzekwa, K. R.; Krishnamachary, N.; Shou, M.; Ogai, A.; Parise, R. A.; Rettie, A. E.; Gonzalez, F. J.; Tracy, T. S. *Biochemistry* **1998**, *37*, 4137−4147.
(12) Ueng, Y. F.; Kuwabara, T.; Chun, Y. J.; Guengerich, F. P. *Biochemistry* **1997**, *36*, 370−381.
(13) Miller, G. P.; Guengerich, F. P. *Biochemistry* **2001**, *40*, 7262−7272.
(14) Atkins, W. M. *Drug Discovery Today* **2004**, *9*, 478−484.
(15) Harlow, G. R.; Halpert, J. R. *Proc. Natl. Acad. Sci. U.S.A.* **1998**, *95*, 6636−6641.
(16) Schrag, M. L.; Wienkers, L. C. *Drug Metab. Dispos.* **2000**, *28*, 1198−1201.
(17) Atkins, W. M.; Wang, R. W.; Lu, A. Y. H. *Chem. Res. Toxicol*. **2001**, *14*, 338−347.
(18) Roberts, A. G.; Campbell, A. P.; Atkins, W. M. *Biochemistry* **2005**, *44*, 1353−1366.
(19) Baas, B. J.; Denisov, I. G.; Sligar, S. G. *Arch. Biochem. Biophys.* **2004**, *430*, 218−228.

in CYP3A4 and P450eryF. Using these methods, a stoichiometry of 1:1 for the binding of bromocriptine to CYP3A4 and 1:2 for the binding of 1-PB to CYP3A4 and pyrenemethylamine to P450eryF was determined.[22,23]

To circumvent some of the complications inherent in studying CYP3A4, the soluble bacterial P450eryF has been utilized in numerous studies as a model system of an allosteric enzyme. The mechanism of cooperativity in P450eryF has been studied using a variety of techniques such as X-ray crystallography, FRET, site-specific mutagenesis, UV−vis spectroscopy, and NMR.[2,24−29] Our laboratory recently determined affinities of the two binding sites for the allosteric substrate 1-PB at two different ligand-enzyme ratios, and a sequential binding mechanism was proposed.[28] Recently, NMR methods were used to probe the mechanism of cooperativity exhibited by P450eryF upon 9-AP (type-II) or testosterone (type-I) binding.[29] Both compounds perturbed the same phenylalanine residues, suggesting the presence of two "binding niches" within a large binding pocket, remarkably consistent with the crystal structures.[2] On the basis of the simulated values of two binding constants, positive homotropic and negative homotropic cooperativity were suggested for 9-AP and testosterone, respectively.[29] Our previous spectral studies with P450eryF suggested positive cooperativity for testosterone.[25] However, it is not apparent either from crystal structures or from NMR studies which site is the high or low affinity one in P450eryF. In the case of testosterone, Roberts et al. observed that interaction at the high affinity binding site was able to elicit a change in spin state, suggesting binding closer to heme.[29] Conversely, our studies with 1-PB showed that the low-to-high spin shift occurred only upon binding of a second molecule to a lower affinity site, at least at low ionic strength.[28] The molecular details of the mechanism of allostery require further elucidation to understand the interplay and nature of these binding sites. Hence, it is essential to directly measure the two binding constants and the associated energetics in a single experiment using ligands of varying chemistry and also to determine/assign the location based on the energetic compatibility. Isothermal titration calorimetry (ITC) is the method of choice to examine the complete thermodynamics of protein−ligand interactions in solution, because ITC directly measures the enthalpy of bi-molecular interaction and is independent of the accompanying spectroscopic changes. This method is being extensively and successfully used in combination with structural information as a major tool in structure-based drug discovery research in a variety of systems.[30−32] Recent advances in calorimetric sensitivity and data analysis have enabled innovative solution conditions to be applied to the protein−ligand system.[32−37] Recently we employed ITC for the first time to the P450 system to monitor the solution thermodynamics of ligand interaction in CYP2B4.[38] The remarkable flexibility of the CYP2B4 active site in binding inhibitors of different ring chemistry and side chain was elucidated using the thermodynamic signature derived from ITC in conjunction with X-ray crystal structures.[4,5,9,38]

Here we use ITC to dissect the stoichiometry and energetics of P450eryF cooperativity using ligands of diverse chemistry: three bulkier ligands (1-PB, 9-AP, and ANF) and two smaller ligands (4-PP and 4-CPI) that induce either type-I or type-II spectral changes. 4-PP and 4-CPI showed only one binding site, whereas the three bulkier ligands showed perfect 2:1 binding stoichiometry. The results revealed 2-fold greater binding affinity at the first site than at the second site and were consistent with a sequential binding mechanism. The Hill coefficients derived by spectral titrations were >1.7 for the three bulkier ligands, indicating the prominent allostery. Competitive binding studies confirmed that all these ligands bind to the same binding pocket but with different affinity. The binding events for 1-PB were strongly hydrophobic and driven by favorable entropy, whereas 9-AP and ANF interactions were enthalpically driven. Molecular docking simulations were used to localize the sites and assign thermodynamic signatures derived from ITC, showing the flexibility of the binding pocket residues in accommodating two allosteric ligands in two sub-sites of a large and rigid binding pocket to bring about allostery.

Materials and Methods

Materials. TCEP, EDTA, PMSF, 9-AP, ANF, 4-PP (Sigma-Aldrich Chemical Co., St Louis, MO), 1-PB (Molecular Probes Inc., Eugene, OR), and 4-CPI (Maybridge Chemical Co., Cornwall, UK) were used as obtained. All the other chemicals used were of analytical grade.

Protein Expression and Purification. P450eryF and the P450eryF (S93C/C154S) mutant were expressed in *Escherichia coli*[24,28] and purified as described previously for CYP2B4[38] with minor modifications. Briefly, the protein was extracted in 20 mM HEPES buffer containing 1 mM DTT, 1 mM EDTA, 500 mM NaCl, 1 mM PMSF, and 20% glycerol, pH 7.4. Protein-bound Ni-NTA resin was washed twice with the above buffer (without EDTA) and the buffer containing 20 mM histidine, and eluted with 50−70 mM of histidine. The fractions having an A_{417}:A_{280} ratio above 1.8 were subjected to SDS-PAGE and pooled according to homogeneity. The protein was dialyzed extensively against the buffer (without PMSF) to remove histidine and stored at −80 °C after flash freezing in liquid nitrogen. Glycerol was removed, and DTT was exchanged for 1 mM TCEP by extensive dialysis. All subsequent experiments were performed in 20 mM HEPES buffer containing 1 mM TCEP and 500 mM NaCl, pH 7.4, unless otherwise

(20) Davydov, D. R.; Fernando, F.; Baas, B. J.; Sligar, S. G.; Halpert, J. R. *Biochemistry* **2005**, *44*, 13902−13913.
(21) Koley, A. P.; Buters, J. T.; Robinson, R. C.; Markowitz, A.; Friedman, F. K. *J. Biol. Chem. 272*, 3149−3159.
(22) Davydov, D. R.; Fernando, F.; Halpert, J. R. *Biophys. Chem.* **2006**, *123*, 77−83.
(23) Fernando, F.; Halpert, J. R.; Davydov, D. R. *Biochemistry* **2006**, *45*, 4199−4209.
(24) Khan, K. K.; Liu, H.; Halpert, J. R. *Drug Metab. Dispos.* **2003**, *31*, 356−359.
(25) Khan, K. K.; He, Y. A.; He, Y. Q.; Halpert, J. R. *Chem. Res. Toxicol.* **2002**, *15*, 843−853.
(26) Davydov, D. R.; Kumar, S.; Halpert, J. R. *Biochem. Biophys. Res. Commun.* **2002**, *294*, 806−812.
(27) Davydov, D. R.; Botchkareva, A. E.; Kumar, S.; He, Y. Q.; Halpert, J. R. *Biochemistry* **2004**, *43*, 6475−6485.
(28) Davydov, D. R.; Botchkareva, A. E.; Davydova, N. E.; Halpert, J. R. *Biophys. J.* **2005**, *89*, 418−432.
(29) Roberts, A. G.; Diaz, M. D.; Lampe, J. N.; Shireman, L. M.; Grinstead, J. S.; Dabrowski, M. J.; Pearson, J. T.; Bowman, M. K.; Atkins, W. M.; Campbell, A. P. *Biochemistry* **2006**, *45*, 1673−1684
(30) Leavitt, S.; Freire, E. *Curr. Opin. Struct. Biol.* **2001**, *11*, 560−566.
(31) Lopez, M. M.; Makhatadze, G. I. *Methods Mol. Biol.* **2002**, *173*, 121−126.
(32) Weber, P. C.; Salemme, F. R. *Curr. Opin. Struct. Biol.* **2003**, *13*, 115−121.
(33) Muralidhara, B. K.; Wittung-Stafshede, P. *Biochemistry* **2003**, *42*, 13074−13080.
(34) Muralidhara, B. K.; Chen, M.; Ma, J.; Wittung-Stafshede, P. *J. Mol. Biol.* **2005**, *349*, 89−97.
(35) Ohtaka, H.; Velazquez-Compoy, A.; Xie, D.; Freire, E. *Protein Sci.* **2002**, *11*, 1908−1916.
(36) Turnbull, W. B.; Daranas, A. H. *J. Am. Chem. Soc.* **2003**, *125*, 14859−14866.
(37) Muralidhara, B. K.; Wittung-Stafshede, P. *Biochemistry* **2004**, *43*, 12855−12864.
(38) Muralidhara, B. K.; Negi, S.; Chin, C. C.; Braun, W.; Halpert, J. R. *J. Biol. Chem.* **2006**, *281*, 8051−8061.

noted. The P450 concentration was measured by reduced CO difference spectra using an extinction coefficient of 91 mM^{-1} cm^{-1}.

Analytical Ultracentrifugation Experiments. Sedimentation velocity runs were performed using a Beckman-Coulter model XLA analytical ultracentrifuge at 60 000 rpm and 20 °C, as described previously[38] but in the absence of detergent. Ligand-free or ligand-bound P450eryF was loaded into two different 3 mm double sector quartz cells with a respective blank sector containing buffer and equal concentration of ligand. Samples were spun at 60 000 rpm and were monitored simultaneously at 417 and 280 nm. A 60 μM protein concentration and a 2-fold molar excess of ligands were used. Partial specific volumes, solvent density, and viscosity were calculated using SEDNTERP program.[39]

Ligand Binding by Equilibrium UV−Vis Difference Spectral Titration. Difference spectra were recorded using 2 μM of P450eryF on a Shimadzu-2600 spectrophotometer at 25 °C. Protein sample (3 mL) was divided into two matched quartz cuvettes, and a baseline was recorded between 350 and 500 nm. Difference spectra were recorded following the addition of a series of 2 μL aliquots of ligand (stock concentration was 1 mM of 9-AP, 2 mM each of 1-PB and ANF, all in ethanol; 1 mM each of 4-CPI and 4-PP in 2.5% ethanol) to the sample cuvette and the same amount of ethanol to the reference cuvette. For the competitive binding experiments, P450eryF was saturated with a 20- to 30-fold molar excess of 1-PB, ANF, or 9-AP before titrating against the competing ligand. The S_{50} and Hill coefficient were obtained by a fit of differential absorbance to the Hill equation in the case of 9-AP, 1-PB, and ANF, whereas the data were fit to the Michaelis−Menten equation to derive K_S in the case of 4-CPI and 4-PP (KaleidaGraph, Synergy Software).

Isothermal Titration Calorimetric (ITC) Experiments and Data Analysis. ITC experiments were performed on a VP−ITC calorimeter interfaced with a computer for data acquisition and analysis using Origin 7 software (Microcal Inc., Northampton, MA) as described previously for CYP2B4-ligand interactions[38] but with modifications in the titration mode and data analysis. Here the experiments were carried out in two different titration modes. In the direct titration mode, more soluble ligands (2 mM of 4-CPI or 4-PP) were placed in the syringe and titrated against P450eryF (60 μM) in the sample cell. In the reverse titration mode, the sparingly soluble ligand (30−50 μM of 9-AP, 1-PB, and ANF) was placed in the sample cell and titrated with P450eryF (500 μM) in the titration syringe. A typical titration schedule included addition of 3−4 μL per injection of titrant with 20−30 injections spaced at 4−5 min intervals. The titration syringe was continuously stirred at 305 rpm, and the cells were thermostated at 25 °C. For the first injection only, 0.5−1 μL of titrant was added, and the corresponding data point was deleted from the analysis. Reference titrations were carried out by injecting each titrant (either ligand or protein) into buffer alone in the calorimetric cell, and heat of dilution was subtracted from the protein−ligand titration data.

The binding isotherm for 4-PP was also obtained in the reverse titration mode by titrating P450eryF into 4-PP in the sample cell. The data obtained both in "direct" and "reverse" titration modes were best fit to single-class of binding sites model yielding perfect 1:1 stoichiometry ($N = 1$) and similar thermodynamic parameters. The binding isotherms of 9-AP, 1-PB, and ANF were fit to a single-class of binding site models to accurately determine the stoichiometry (N). The known cooperative binding nature of these ligands from spectral studies enabled curve-fitting of the data using a two-site sequential binding model to determine the thermodynamic parameters for the two interacting sites. Otherwise, if the two binding sites are non-identical, calorimetric studies alone cannot determine whether the sites are independent or interacting.[40,41] In addition, a curve fit to a two-independent classes of binding site model or a sequential binding model for more than two sites yielded unreasonable errors in the thermodynamic parameters. For the competitive binding studies, the protein was preloaded with ligand (1-PB or ANF) to 2:1 stoichiometry before titrating into the competing ligand (9-AP) in the sample cell, and data were analyzed using a sequential binding model. Similar thermodynamic parameters were obtained for 4-PP binding in both direct and reverse titration modes using P450 concentrations derived from CO-difference spectra, confirming that only P450 (≥95%) out of total hemoprotein is actively involved in ligand binding, similar to prior results with CYP2B4.[38]

Molecular Docking Simulations. A homology model of the 9-AP-bound P450eryF mutant structure was built with MODELLER[42] by replacing Ser-93 with Cys and Cys-154 with Ser and showed an rmsd of 0.24 Å. The structure was energy minimized using 30 000 steps of NAMD[43] to remove bad steric contacts. The final structure, which showed an rmsd of 0.84 Å with the original structure (pdb: 1EGY), was used for docking simulations. Automated docking simulation of ligands was performed using AUTODOCK 3.0.5 to search for the minimum energy conformations and the ligand orientations according to the Lemarckian Genetic Algorithm.[44] Kollman-united atom charges were assigned to the protein using AUTODOCKTOOLS, and the charges for the heme were assigned as described previously.[45] Docking simulations were also performed on the original structure (pdb: 1EGY) by removing the two bound 9-AP molecules. All ligands (9-AP, 1-PB, ANF, 4-CPI, and 4-PP) were docked sequentially to the structure using two 40 × 40 × 40 point grids with a spacing of 0.375 Å, centered around the nitrogen of bound 9-AP molecules at −8.8,10.5,11.5 Å for the first site (closer to heme) and −13.1,10.2,16.9 Å for the second site (away from heme). The larger grid used allows torsional flexibility of a ligand to find the minimum energy position, since the protein flexibility is limited and the decrease in the grid size did not alter the docking conformation or energy. The first docked molecule of the minimum energy ensemble was always retained within the grid while docking the second ligand. A total of 5−10 unique minimum energy ensembles that exhibited less than 1.0 Å in positional rmsd were selected for each ligand at both sites, and the lowest energy configuration was selected for further analysis. Docking of ligands to the first and the second sites showed one major conformation with lowest energy for all the ligands, although the energy differences between the top two clusters of allosteric ligands at the second site was minimal (∼0.3 kcal/mol). Amino acid side chains within 4 Å of the docked positions were mapped. Molecular structures of ligands were modeled and the charges were assigned using PRODRG server[46] (davapc1.bioch.dundee.ac.uk/programs/prodrg/).

Results

ITC and Spectral Studies with Ligands that Exhibit No Cooperativity. All the experiments in this study were performed using a P450eryF (S93C/C154S) mutant that retains the key functional properties of the wild type and exhibits similar cooperativity.[28] Besides imidazoles, pyridines are another prominent class of nitrogen heterocycles that show type-II binding with P450s. Here we have used 4-PP and 4-CPI as representative small compounds from each class to characterize the binding interactions. Binding of these ligands to P450eryF induced type−II spectral changes characterized by an absorbance minimum at 413 nm and a maximum at 431 nm, which is

(39) Lebowitz, J.; Lewis, M. S.; Schuck, P. *Protein Sci.* **2002**, *11*, 2067−2079.
(40) Wiseman, T.; Williston, S.; Brandts, J. F.; Lin, L-N. *Anal. Biochem.* **1989**, *179*, 131−137.
(41) Dam, T. K.; Roy, R.; Page, D.; Brewer, C. F. *Biochemistry* **2002**, *41*, 1359−1363.
(42) Sali, A.; Blundell, T. L. *J. Mol. Biol*. **1993**, *234*, 779−815.
(43) Kalé, K.; Skeel, R.; Bhandarkar, M.; Brunner, R.; Gursoy, A.; Krawetz, N.; Phillips, J.; Shinozaki, A.; Varadarajan, K.; Schulten, K. *J. Comput. Phys.* **1999**, *151*, 283−312.
(44) Morris, G. M.; Goodsell, D. S.; Halliday, R. S.; Huey, R.; Hart, W. E.; Bellew, R. K.; Olson, A. J. *J. Comput. Chem.* **1998**, *19*, 1639−1662.
(45) Helms, V.; Wade, R. C. *Biophys. J.* **1995**, *69*, 810−824.
(46) van Aalten, D. M.; Bywater, R.; Findlay, J. B.; Hendlich, M.; Hooft, R. W.; Vriend, G. *J. Comput. Aided Mol. Des.* **1996**, *10*, 255−262.

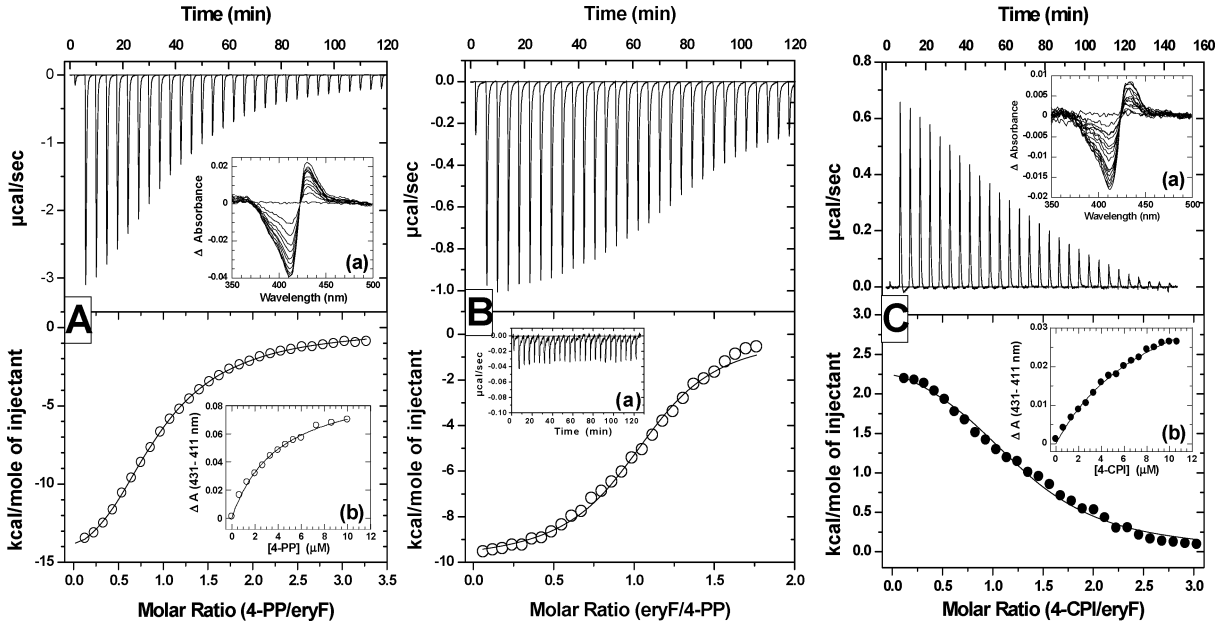

Figure 1. Calorimetric and spectral binding studies with 4-PP and 4-CPI. Calorimetric enthalpy signals (upper panel) and the resulting binding isotherm (lower panel) are shown for direct (A) (4-PP in syringe) and reverse (B) (4-PP in cell) titration of 4-PP with P450eryF. The 4-CPI titration (direct) is shown in C. The binding isotherm was best fit to single-class of binding site model (solid line) yielding 1:1 stoichiometry in all the cases. Type−II difference spectra upon binding (Inset a) and the resulting binding data fit to Michaelis−Menten equation (Inset b) are shown for 4-PP and 4-CPI in A and C, respectively. The binding parameters obtained are listed in Table 1. The calorimetric heat of dilution upon injecting 4 μL each of 0.6 mM P450eryF to the buffer in the calorimetry cell is shown as Inset (a) of B, indicating no possible protein oligomer formation at 0.5−0.6 mM protein concentration used in the reverse titrations.

indicative of nitrogen ligation to the heme iron as shown in inset a of Figure 1A and Figure 1C for 4-PP and 4-CPI, respectively. A plot of differential absorbance vs ligand concentration is shown as inset b of the respective figures. The K_S values were 4.2 and 9.4 μM for 4-PP and 4-CPI, respectively. The ΔA_{max} for 4-PP binding was almost 2-fold higher than that observed for 4-CPI binding.

Prior to ITC experiments to determine the thermodynamic parameters of ligand binding, the monomeric state of P450eryF at high concentration (60 μM) was confirmed by sedimentation velocity experiments with and without various ligands used in this study. A representative pattern is shown with an S value of 3.1 $\pm$ 0.1 for ligand-free and 9AP-bound forms (Figure S1, Supporting Information). All sedimentation experiments were simultaneously monitored at 280 nm, yielding similar results as the measurements at 417 nm. The monomeric state at high protein concentration (0.5−0.6 mM) was confirmed indirectly from the lack of heat of probable protein dissociation observed when protein at high concentration (0.6 mM) was titrated against buffer in the calorimetric cell, as shown in inset a of Figure 1B. The enthalpic changes were similar to buffer−buffer titrations.

The calorimetric data for 4-PP and 4-CPI binding to P450eryF are shown in Figures 1A and C, respectively. A typical calorimetric titration, which consisted of adding 4 μL aliquots of 2 mM ligand to 60 μM of P450eryF at 25 °C, together with the nonlinear least-squares fit of the data are shown. The upper panels in each figure exhibit a monotonic decrease in the heat of binding (exothermic with 4-PP and endothermic with 4-CPI) with successive injections until saturation is reached. The lower panels show the integrated enthalpic changes for each injection, which fit to the single-class of binding-site model (solid line). Fitting of integrated enthalpic data to two-classes of binding-site models or to a two-site sequential binding-site model each yielded unreasonable error in stoichiometry and thermodynamic parameters. The results of ITC experiments are summarized in Table 1. A clear 1:1 stoichiometry was observed for both 4-PP and 4-CPI with the respective K_D values of 15 and 28 μM. Striking differences were seen in the energetics, as 4-PP binding is enthalpically driven ($\Delta H = -19$ kcal/mol), whereas 4-CPI is entropically favorable ($\Delta S = 41$ cal/mol/K).

The allosteric ligands used in this study were sparingly soluble, and hence it was necessary to standardize the reverse titrations keeping the ligand in the cell and protein in the syringe. This approach was first validated with 4-PP. A typical reverse titration involving injection of 4 μL aliquots of 500 μM P450eryF to 40 μM of 4-PP in the cell at 25 °C (upper panel), together with the nonlinear least-squares fit of the enthalpy data to "single-class of binding site" model (lower panel) are shown in Figure 1B. A clear 1:1 stoichiometry with similar thermodynamic parameters as the direct titrations was obtained, as shown in Table 1.

ITC and Spectral Studies with Ligands that Exhibit Varying Degrees of Cooperativity. Binding of 9-AP to P450eryF induced a type−II spectral change, whereas 1-PB and ANF binding yielded a type-I spectral change, as shown in inset a of Figure 2A, B, and C, respectively. The plots of differential absorbance (peak and trough) against ligand were sigmoidal and were fit to the Hill equation. The S_{50} and Hill coefficient values derived for 9-AP, 1-PB, and ANF binding were 2.9, 4.9, 9.8 μM, and 1.75, 1.98, 1.85, respectively.

The number of binding sites and the associated thermodynamic parameters were directly determined using ITC in the reverse mode, as shown in Figure 2A, B, and C, respectively, for 9-AP, 1-PB, and ANF. The upper panels exhibit a monotonic decrease in the heat of interaction (exothermic for 9-AP and ANF, endothermic for 1-PB) with successive injections until saturation is reached. The lower panels show the integrated

Table 1. Thermodynamic Parameters of Ligand Interaction with P450eryF Derived from ITC and Spectral Titrations

	isothermal titration calorimetry					spectral titrations	
ligand	N^a	$K_a \times 10^{-4}$ (M^{-1})	ΔG^d (kcal/ mol)	ΔH (kcal/ mol)	ΔS^e (cal/ mol/ K)	Hill coefficient	S_{50} or K_S (μM)
4-PP						−	4.2 ± 0.3
direct	0.98 ± 0.02	6.4 ± 0.2	−6.5 ± 0.1	−18.8 ± 1.4	−41.1 ± 2.5		
reverse	0.95 ± 0.07	8.2 ± 0.5	−6.7 ± 0.3	−16.5 ± 1.9	−39.1 ± 2.9		
4-CPI	1.15 ± 0.08	3.6 ± 0.2	−6.2 ± 0.3	6.0 ± 1.0	41.0 ± 2.8	−	9.4 ± 1.0
ANF	2.0 ± 0.1					1.85 ± 0.14	9.8 ± 0.2
ANF_1		8.3 ± 0.5	−6.7 ± 0.3	−16.6 ± 3.5	−33.2 ± 3.5		
ANF_2		3.7 ± 0.5	−6.2 ± 0.3	7.0 ± 2.5	44.5 ± 5.5		
1-PB	1.9 ± 0.1					1.98 ± 0.11	4.9 ± 0.1
1-PB_1		9.8 ± 3.5	−6.8 ± 0.3	3.9 ± 0.1	35.9 ± 2.4		
1-PB_2		4.1 ± 0.4	−6.3 ± 0.3	4.3 ± 0.1	35.5 ± 2.5		
9-AP	2.1 ± 0.1					1.75 ± 0.06	2.9 ± 0.1
9-AP_1		19.5 ± 0.4	−7.2 ± 0.3	−5.3 ± 0.2	6.4 ± 1.5		
9-AP_2		9.1 ± 0.2	−6.7 ± 0.3	−6.2 ± 1.5	1.9 ± 0.1		
9-AP[b]	2.0 ± 0.1					2.04 ± 0.21	3.2 ± 0.1
9-AP_1[b]		4.6 ± 0.5	−6.4 ± 0.5	−6.3 ± 2.5	−0.36 ± 0.02		
9-AP_2[b]		7.2 ± 0.5	−6.6 ± 0.6	−5.8 ± 2.5	2.56 ± 0.02		
9-AP[c]	2.2 ± 0.1					1.83 ± 0.06	1.5 ± 0.1
9-AP_1[c]		1.4 ± 0.1	−5.7 ± 0.1	−87 ± 11	−275 ± 15		
9-AP_2[c]		0.2 ± 0.1	−4.6 ± 2.2	−167 ± 57	−547 ± 125		

[a] Obtained by a curve fitting to a single class of binding sites model. [b] 9-AP binding to P450eryF prebound with ANF. [c] 9-AP binding to P450eryF prebound with 1-PB. [d] $\Delta G = -RT \ln K_a$. [e] $\Delta S = (\Delta H - \Delta G)/T$.

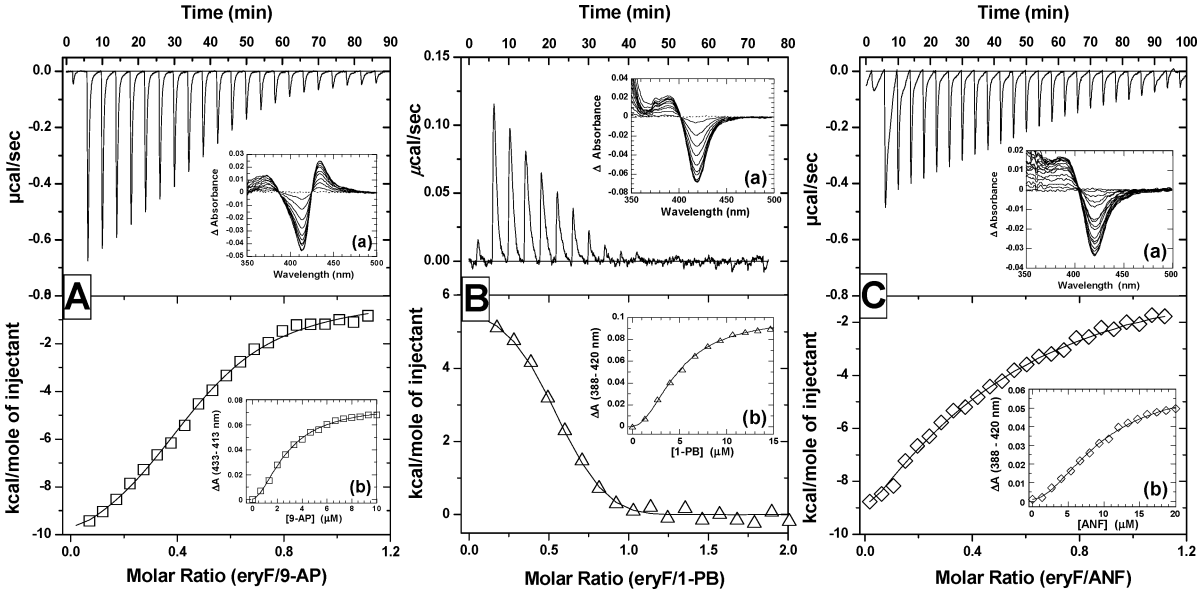

Figure 2. Calorimetric binding data of 9-AP (A), 1-PB (B), and ANF (C) with respective spectral data as insets. The calorimetric enthalpy changes (upper panel) and the resulting integrated enthalpy data (lower panel) fit to a sequential two-site binding model (solid line) are shown. Only 1-PB binding is endothermic. All titrations were carried out in the reverse-mode keeping the ligand in the cell and the P450eryF in the syringe (see Methods for details). The equilibrium difference spectra (Inset a) show type-II binding for 9-AP and type-I binding for both 1-PB and ANF. The spectral data were fit to the Hill equation, yielding a sigmoidal pattern (Inset b) indicative of cooperative ligand binding. The binding parameters obtained from ITC and spectral titrations are listed in Table 1.

enthalpic changes for each injection, which fit to a "sequential binding sites" model (solid lines) with two sites. Fitting of enthalpic data to a simple "two sets of independent sites" model yielded a poor fit with unreasonable error in the stoichiometry and thermodynamic parameters. In addition, although studies performed at lower ionic strength (I = 0.029 M) verified the 2:1 stoichiometry of 9-AP, 1-PB, and ANF, clear evaluation of the interaction thermodynamics was not feasible due to the complex nature of the binding isotherms (data not shown).

The absence of biphasicity in the binding curves of interaction enthalpy with 9-AP, 1-PB, and ANF indicates cooperativity between the two ligand binding sites, although it is not very apparent from the calorimetric data alone.[40] The dissociation constants obtained are 5 and 11 μM for 9-AP_1 and 9-AP_2, 10 and 24 μM for 1-PB_1 and 1-PB_2, and 12 and 27 μM for ANF_1 and ANF_2. Only in the case of 9-AP were both enthalpy and entropic changes favorable for binding at both the sites. The asymmetric titration peaks with large peak area observed for each injection of 1-PB and ANF (upper panels of Figure 2B and C) in contrast to 9-AP (upper panel of Figure 2A) reflect a weak and slow binding process. The binding parameters obtained are listed in Table 1, and the thermodynamic signatures dissected for the two sequential binding sites along with the single-binding site ligands (4-CPI and 4-PP) are shown in Figure 3. The chemical structure of the respective ligand is also included. All three allosteric ligands are structurally planar and have minimal or no flexibility, with the number of rotatable bonds being 0, 1, and 3 for 9-AP, ANF, and 1-PB, respectively.

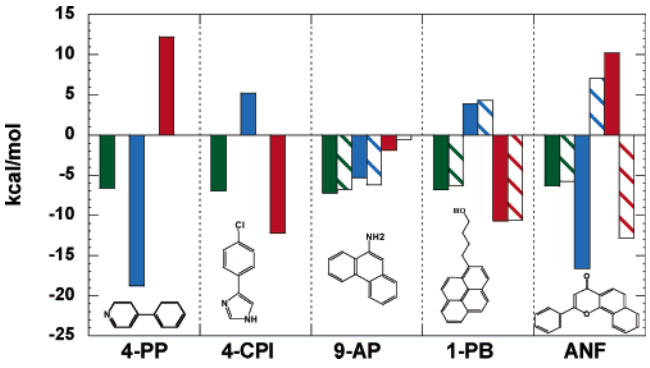

Figure 3. Thermodynamic signatures of ligand binding. The ΔG (green), ΔH (blue) and $-T\Delta S$ (red), obtained for ligand binding site/s (site 1: solid bar, site 2: crossed bar) on P450eryF by ITC experiments are shown for different ligands. The data were obtained from the fit of a sequential two-site binding model for 9-AP, 1-PB, and ANF and single-site model for 4-PP and 4CPI. The chemical structures of ligands (ChemDraw Ultra 7.0, Cambridgesoft) are shown in respective insets.

Competitive Ligand Binding to the Allosteric Sites. Several crystal structures of P450eryF have showed the existence of two ligand molecules bound to the protein, although there is no structural evidence that the binding site would accommodate two dissimilar ligands.[2,47,48] As 9-AP binds with lower K_D and more favorable energetics than 1-PB or ANF (Table 1), we examined 9-AP binding to P450eryF presaturated with 1-PB or ANF and monitored the spectral and enthalpic changes as shown in Figure 4A and B, respectively. Binding of 9-AP to P450eryF presaturated with ANF also induced a type-II spectral change (Figure 4A, inset a-1) with a ΔA_{max} similar to that observed for 9-AP binding to unliganded protein (Figure 2A, inset a). The resulting binding curve also exhibits cooperativity with a Hill coefficient of 2.04 and a S_{50} value of 3.2 μM (Figure 4A, inset a-3). Conversely, when ANF (weaker binder) was competed with P450eryF presaturated with 9-AP, no type-I change was observed (Figure 4A, inset a-2) in contrast to unliganded protein (Figure 2C, inset a). Competitive binding of 9-AP to the protein presaturated with 1-PB did induce a typical type-II change (Figure 4B, inset b-1) but with large spectral interference from the type-I change caused by the prebound 1-PB. The resulting binding curve also showed a sigmoidal pattern (Figure 4B, inset b-3). In contrast, 1-PB did not induce any significant type-I spectra when competed with P450eryF prebound with 9-AP (Figure 4B, inset b-2). However, competitive binding of 1-PB to the protein prebound with ANF showed a type-I spectra and a sigmoidal binding curve with the Hill coefficient and S_{50} values of 1.3 and 8.5 μM, respectively (Figure S2, Supporting Information). ANF binding to protein prebound with 1-PB showed only minor spectral changes.

Competitive binding studies using ITC were feasible only with 9-AP, as the binding of this ligand to the protein saturated with either ANF or 1-PB produced reliable interaction enthalpy and good binding isotherms. A typical calorimetric profile of 1-AP binding to P450eryF saturated either with ANF or 1-PB is shown in Figure 4A and B, respectively. The upper panels represent the monotonic decrease in the enthalpy of interaction with the increase in protein (prebound with ANF or 1-PB) concentration, and the lower panels represent the integrated binding enthalpy fit to a "sequential binding site" model with two sites. The binding enthalpy for each injection in the case that of P450eryF-ANF complex was almost 2-fold lower than observed with the unliganded protein titrated with 9-AP (Figure 2A), clearly indicating competition for the same binding pocket. However, the cumulative enthalpy of the two sites remained similar with decreased free energy and was compensated largely by unfavorable entropy (Table 1). The K_D for 9-AP$_1$ was increased to 21 and 71 μM, respectively, in P450eryF prebound with ANF and 1-PB. The respective values for the 9-AP$_2$ were 14 and 500 μM. The enthalpy−entropy compensation values for the competitive binding are listed in Table 1, which clearly indicate the competition of allosteric ligands for the same binding pocket irrespective of the ligands being type-I or type-II binders.

Molecular Docking Simulations. The ITC experiments clearly demonstrated two binding sites for allosteric ligands but do not indicate which site is closer to the heme. We performed docking simulations to probe and assign the possible structural location of the two binding sites for 9-AP, 1-PB, and ANF. To evaluate the accuracy of the AutoDock program in predicting the ligand binding modes at allosteric sites of P450eryF, we examined the relative positions of two docked 9-AP molecules with respect to the bound conformations of 9-AP in the X-ray crystal structure at the first (closer to heme) and second (away from heme) sites. (pdb: 1EGY). The two 9-AP molecules were sequentially docked and differed with an rmsd of only 0.5 Å at the first site and 2.2 Å at the second site from the location seen in the crystal structure (data not shown). We used the homology model of the S93C/C154S mutant (used in all the solution studies) as a docking template. It differed from the original structure with an rmsd of only 0.83 Å. The homology model superimposed on the original structure and the relative position of the two large 40 × 40 × 40 grids placed at the distal end of the heme used for docking simulation are shown in Figure 5A. The first 9-AP molecule was docked in a perfect conformation with the free nitrogen of 9-AP facing the heme iron at 2.05 Å distance, which is favorable for producing a type-II spectral change. The docked 9-AP conformation was similar to the one seen in the first site of the crystal structure with the same contact residues. The second 9-AP molecule was then docked and assumed a favorable conformation slightly different from the one seen in the crystal structure at the second site (about 4 Å shifted toward the I-helix). A representative position of 9-AP from an ensemble of minimum energy conformations at the first and second site are shown in Figure 5B, and the surrounding residues within 4 Å distance are listed in Table S3 (Supporting Information).

The minimum energy conformation for 1-PB at the first site was 2.92 Å from the heme iron, and the plane of pyrene ring was at about a 20° angle with the heme plane, favorable for van der Waals contacts. The butanol side chain makes contact with Val-237 and Leu-238 on the I-helix, which is favorable for a strong hydrophobic interaction. The second 1-PB molecule was docked almost parallel to the heme plane at a distance of 4.5 Å from the heme iron and interacts with three hydrophobic residues (Val-237, Leu-391, and Leu-392). Interestingly, the 1-PB docked at the second site lies almost parallel at 2.8 Å

(47) Cupp-Vickery, J. R.; Garcia, C.; Hofacre, A.; McGee-Estrada, K. *J Mol. Biol.* **2001**, *311*, 101−110.
(48) Nagano, S.; Cupp-Vickery, J. R.; Poulos, T. L. *J. Biol. Chem.* **2005**, *280*, 22102−22107.

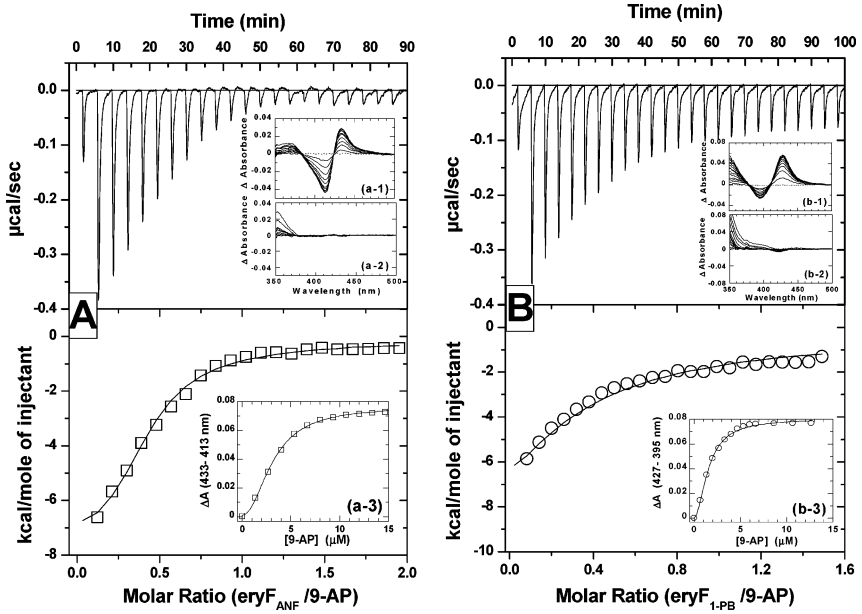

Figure 4. ITC and spectral studies of competitive ligand binding to P450eryF. The calorimetric enthalpy changes (upper panel) and the resulting integrated enthalpy data (lower panel) fit to a sequential two-site binding model (solid line) for 9-AP binding to P450eryF prebound with ANF (A) or 1-PB (B) to 2:1 stoichiometry are shown. The corresponding equilibrium difference spectra (Inset a-1, b-1) and resulting binding data fit to the Hill equation (Inset a-3, b-3) are shown. In the reverse spectral titration, the binding of ANF to P450eryF prebound with 9-AP (Inset a-2) and 1-PB to P450eryF prebound with 9-AP (Inset b-2) did not induce significant spectral changes. The binding parameters obtained are listed in Table 1.

distance above the 1-PB molecule docked at the first site favoring strong hydrophobic π-stacking interactions. A representative position of 1-PB from an ensemble of minimum energy conformations at the first and second sites is shown in Figure 5C. Docking of the first molecule of ANF produced a minimum energy conformation similar to 9-AP but at a distance of 2.98 Å from the heme iron. The location and conformation of this ANF molecule result in possible interactions with all the 9-AP binding residues and additional nonhydrophobic residues of the B−C loop. However, ANF docked at the second site was farthest of all ligands (5.9 Å from heme iron and heme plane) and positioned almost perpendicular to the first ANF molecule with very strong hydrophobic interaction with more than six very hydrophobic residues. A representative position of ANF from an ensemble of minimum energy conformations at the first and second sites is shown in Figure 5D, and the surrounding residues within 4 Å distance are listed in Table S3. The docking free energy of the most favored ligand conformation for the first site was about 1.2 kcal/mol lower than the second site, for all three allosteric ligands.

Docking simulations were performed in a similar way with the two smaller ligands (4-CPI and 4-PP) that showed 1:1 binding stoichiometry and no cooperativity. In both cases, the nitrogen of the first molecule (imidazole of 4-CPI and pyridine of 4-PP) is positioned close to the heme iron. However, the second ligand molecule was docked next to the first ligand in the large space between the I-helix and B−C loop with much lower docking energy. For both the ligands, the tethering effect of contact residues was absent at the first site, as opposed to the allosteric ligands.

Discussion

Cooperativity of P450s in substrate metabolism and ligand binding confounds prediction of drug metabolism and drug−drug interactions. Bacterial P450eryF is the only soluble P450 that exhibits cooperativity and serves as an excellent model to understand the molecular mechanisms of such processes in mammalian systems.[17−29,49,50] Recently, studies from our laboratory and others have utilized various spectroscopic methods to establish ligand binding stoichiometry and binding affinities at two different sites in P450eryF and P450 3A4.[18,23,28,29] Here we report the direct dissection of two dissociation constants and their energetics for either type-I or type-II compounds that exhibit cooperativity and 2:1 binding stoichiometry with P450eryF. The two smaller type-II compounds studied bind only with 1:1 stoichiometry. The thermodynamic data derived using ITC supported by spectral studies of cooperativity were assigned energetically with ligand binding sites from docking simulations.

The thermodynamic signatures derived from ITC experiments are shown in Figure 3. The interaction of 9-AP$_1$ is driven by more favorable enthalpic and entropic contributions compared with 9-AP$_2$, probably as the result of nitrogen coordination to the heme iron. Interaction at 9-AP$_2$ is enthalpically driven with favorable hydrophobic interaction but largely compensated by entropy. The thermodynamic signature of 1-PB$_1$ and 1-PB$_2$ binding is typical of a strong, hydrophobically dominated process with positive enthalpic changes. Binding of ANF$_1$ was an enthalpically favorable, whereas ANF$_2$ was a entropically driven hydrophobic interaction, producing the opposite thermodynamic signature. The K_{D1} (e.g., ANF$_1$) obtained was lower than the K_{D2} (e.g., ANF$_2$) for all three allosteric ligands. The values obtained for 1-PB were higher than the ones obtained previously by FRET-based spectral titrations at low ionic strength.[27,28] Under similar buffer conditions, our S_{50} values determined by spectral titration for all the ligands were also lower than the respective K_D values determined by ITC (Table 1). Such discrepancies between spectral and calorimetric

(49) Yoon, M. Y.; Campbell, A. P.; Atkins, W. M. *Drug Metab. Rev.* **2004**, *36*, 219−230.
(50) Hutzler, J. M.; Hauer, M. J.; Tracy, T. S. *Drug Metab. Dispos.* **2001**, *29*, 1029−1034.

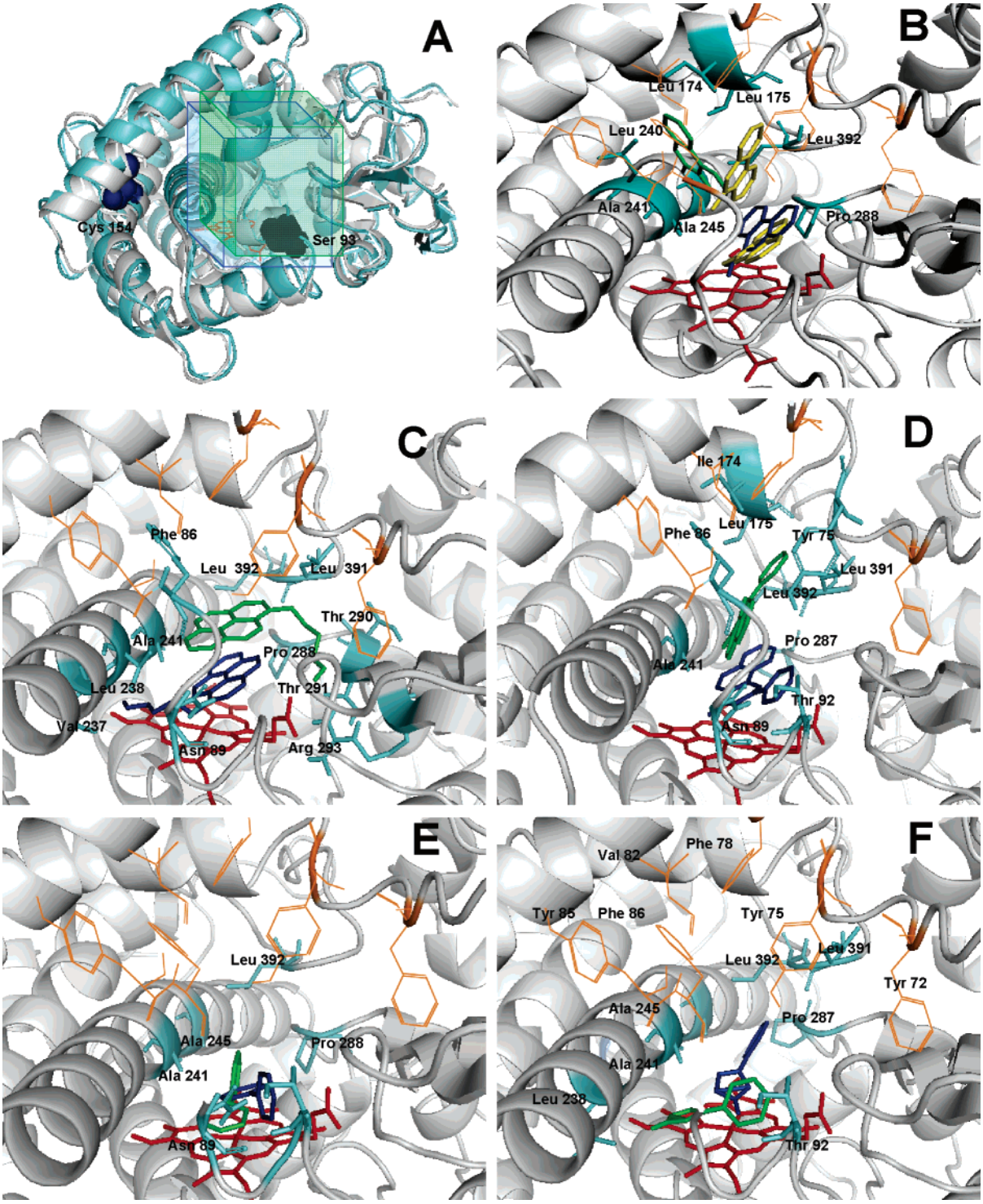

Figure 5. Molecular docking simulations. Structure of P450eryF bound with two 9-AP molecules (pdb: 1EGY) (gray) superimposed on the simulated homology model of P450eryF (S93C/C154S) (green) is shown (A). The structures differ with an rmsd of 0.83 Å and a slightly bent I-helix. The swapped residues, Ser 93 (black) and Cys154 (blue), are indicated. The 40 × 40 × 40 point grids used for docking simulation at the first site (blue) and second site (green) are shown. Using the energy minimized homology model, two molecules of the allosteric ligands, 9-AP (B), 1-PB (C), and ANF (D), and the non-allosteric ligands, 4-PP (E) and 4-CPI (F), were sequentially docked to two sites. A representative conformation from the minimum energy ensemble is shown in each case for the first site (blue) and second site (green). Heme (red), contacts residues (blue), and the hydrophobic cluster on the top of the second site (orange) are shown and are labeled only in (F) for clarity. The original positions of the two 9-AP molecules seen in the crystal structure are also shown (yellow, B) The molecular graphic snap shots were generated using PyMOL.[62]

measurements have been observed in many protein−ligand interaction systems[33,51] including our previous studies of CYP2B4 interaction with seven different imidazole inhibitors.[9,38] Because ITC works on the principle of heat exchange, it measures the cumulative effect of a variety of reactions independent of accompanying spectral and/or spin changes and gives a better picture of the ligand binding process.[33,40,41,51]

(51) Luque, I.; Freire, E. *PROTEINS: Str. Fun. Gen.* **2002**, *49*, 181−190.

Two dissociation constants have been obtained by variety of techniques for binding of several allosteric ligands to P450eryF, and there is also crystallographic and NMR evidence for two binding sites.[2,28,29] However, it is not been possible to draw a correlation in terms of assigning affinities to the location of the binding sites. Although both 1-PB and testosterone are type-I substrates of P450eryF, binding of 1-PB to the high affinity site does not induce a spin transition,[28] whereas an opposite effect was reported for testosterone.[29] This may reflect slight differences in the proximity of the ligand molecule closest to the heme and the ensuing ability to displace the water molecule coordinated as the sixth ligand to heme iron, as clearly shown by a series of crystal structures of P450CAM bound with substrate analogues.[52,53] Alternatively, the high affinity binding of 1-PB may occur at a site much more distal to the heme than in the case of testosterone.

Molecular docking simulations were done to facilitate assignment of the two binding affinities to the probable location on P450eryF. Initially, to evaluate the degree of conformational change upon binding of ligands of different chemistry and size, we calculated the accessible polar and apolar surface area of the one-ligand bound (6-deoxyerythonolide; pdbs: 1OXA, 1Z8O, 1Z8Q and ketoconazole; pdb:1JIN) and two-ligand bound (9-AP; pdb: 1EGY and androstenedione; pdb: 1EUP) forms of P450eryF.[54] Remarkably, the ratio of polar to apolar surface area remained around 41:59 in all cases, in spite of big vs small ligand and one vs two ligand-bound forms. This observation along with the crystallographic data suggests a large and structurally rigid binding pocket of P450eryF,[2] as opposed to the flexible binding pocket observed with CYP2B4 in solution or crystal structures.[4,5,9,38] However, because there is no ligand-free structure of P450eryF, our observations in no way preclude any possible conformational change upon binding of the first ligand molecule. Relative rigidity of the binding pocket can also be evaluated by the comparison of thermodynamic and simulation data of the 4-CPI interaction with P450eryF and CYP2B4. 4-CPI binds weakly to P450eryF ($\Delta\Delta G = 2.1$ kcal/mol) with positive as opposed to the negative enthalpic changes observed in CYP2B4.[38] The spectral titration data showed a more than 2-fold lower ΔA_{max} for 4-CPI binding to P450eryF compared with CYP2B4. In docking simulations, 4-CPI was not clearly tethered by the residues in the binding pocket of P450eryF, similar to 4-CPI docked to the open form of the CYP2B4.[4,38] Interestingly, the 4-CPI docking energies for these two structures were identical (−6.2 kcal/mol) and higher than the perfectly tethered docking (−7.2 kcal/mol) conformation in the closed form of CYP2B4.[5]

In simulations with 9-AP, 1-PB, and ANF, the first ligand was invariably docked near the heme (the first site), whereas the second ligand was more distal (the second site). The interaction of 9-AP at the first site was dominated by the nitrogen-heme iron interaction, whereas binding at the second site involves favorable hydrophobic interaction with four hydrophobic residues and also with the first 9-AP molecule, compatible with the energetics observed for 9-AP_1 and 9-AP_2 in ITC experiments. The positive ΔH is indicative of strong hydrophobic interaction of both 1-PB_1 and 1-PB_2 and is supported by docking results where the first binding site involves close interaction with Val-237 and Leu-238 and the second with Leu-391 and Leu-392 (Table S3). The van der Waals stacking with the heme plane at the first site and a π-stacking interaction between the two 1-PB molecules (2.8 Å distance) adds to the hydrophobicity of the binding sites. Similar pyrene stacking interactions were observed spectroscopically and by the atypical enzyme kinetics of pyrene hydroxylation by CYP3A4.[57,58] Binding of ANF_1 and ANF_2 produced opposite thermodynamic signatures, which correlate nicely with the docked conformations. The first site for ANF is relatively far from the heme plane (4.6 Å) and favorable for hydrophobic interaction with Leu-391 and Leu-392 (Table S3). At the second site, the ANF interaction predominantly involves possible aromatic stacking with the first ANF and the surrounding hydrophobic residues. Calorimetric data also suggest that the interaction of ANF_2 was dominated by an entropically driven hydrophobic interaction. The docking energies are lower for the first site than the second site with all three ligands, also implicating the first site as the high affinity site. These data are consistent with the conclusions from crystallographic and spectral studies that the binding of a second ligand brings about homotropic cooperativity by decreasing the effective size and increasing the hydrophobicity of the large binding pocket.[2,24−29]

The thermodynamic signatures of competitive binding also substantiate a single large binding pocket of P450eryF in solution, where the affinity for 9-AP decreases in the presence of 1-PB or ANF and with a very large unfavorable entropy in the case of displacement of two 1-PB molecules. This competition was difficult to dissect by spectral titration and Hill plot analysis due to overlapping type-I and type-II signals. In the case of 9-AP competing with ANF prebound to P450eryF, the inhibition is reflected by K_D values derived by ITC for the two sites and also the S_{50} values from the Hill plot. The clear competition observed with P450eryF is in contrast to previous observations with CYP3A4[57−59] suggesting a crucial role of the oligomerization and conformational heterogeneity of CYP3A4 in modulating substrate binding.[17−21] The solution thermodynamics and docking simulation data reported here for P450eryF cumulatively suggest that both binding sites are sub-sites of a large single binding pocket. Ionic tethering and electrostatic steering mechanisms were proposed to play an important role in the modulation of substrate and water accessibility, thereby regulating allostery in P450eryF[27] and substrate binding in P450cam[60] and CYP2B4.[61] The lack of cooperativity upon binding of small ligands (4-CPI and 4-PP) to P450eryF (this study) and the very large ligand bromocriptine to CYP3A4[23] suggests the importance of a conformational rearrangement of the binding pocket in cooperativity. Recent NMR studies concluded that testosterone (type-I) and 9-AP (type-II) binding

(52) Raag, R.; Poulos, T. L. *Biochemistry* **1989**, *28*, 917−922.
(53) Raag, R.; Poulos, T. L. *Biochemistry* **1991**, *30*, 2674−2684.
(54) Fraczkiewicz, R.; Braun, W. *J. Comp. Chem.* **1998**, *19*, 319−333.
(55) Dabrowski, M. J.; Schrag, M. L.; Wienkers, L. C.; Atkins, W. M. *J. Am. Chem. Soc.* **2002**, *124*, 11866-11867.
(56) Jushchyshyn, M.; Hutzler, M. J.; Schrag, M. L.; Wienkers, L. C. *Arch. Biochem. Biophys.* **2005**, *438*, 21−28.
(57) Domanski, T. L.; He, Y. A.; Khan, K. K.; Roussel, F.; Wang, Q.; Halpert, J. R. *Biochemistry* **2001**, *40*, 10150−10160.
(58) He, Y. A.; Roussel, F.; Halpert, J. R. *Arch. Biochem. Biophys.* **2003**, *409*, 92−101.
(59) Tsalkova, T. N.; Davydova, N.; Halpert, J. R.; Davydov, D. R. *Biochemistry* **2007**, *46*, 106−119.
(60) Wade, R. C.; Gabdoulline, R. R.; Ludemann, S. K.; Lounnas, V. *Proc. Natl. Acad. Sci. U.S.A.* **1998**, *95*, 5942−5949.
(61) Davydov, D. R.; Hui Bon Hoa, G.; Peterson, J. A. *Biochemistry* **1999**, *38*, 751−761.
(62) Delano, W. L. *The PyMol User's Manual*; Delano Scientific: San Carlos, CA, 2004.

to P450eryF perturbed the same residues, forming two distinct "binding niches" within a single pocket.[29] The favorable entropic changes observed for site 1 (Table 1) with 9-AP and 1-PB reflects local restructuring of the binding pocket, as the entropy derived from the flexibility of these planar ligands is highly limited. A ligand-free structure of P450eryF would certainly be invaluable in clarifying this issue.

In conclusion, we employed the calorimetric approach described previously to study CYP2B4 flexibility in ligand binding to dissect the ligand-binding allostery in P450eryF with sparingly soluble hydrophobic ligands. The thermodynamic interplay between the two-sequential binding sites for allosteric ligands showed the existence of at least two sub-sites within a large binding pocket of P450eryF. Competitive binding studies with 9-AP emphasize that all ligands essentially compete for the same binding pocket and sub-sites. The calorimetric approach described here can be suitably applied to mammalian P450s, especially to CYP3A4 and CYP2C9 in solution or in membrane environment to delineate the implications of stoichiometry and allostery to drug−drug interactions and consequently to develop methods to predict drug incompatibilities.

Abbreviations: 1-PB, 1-pyrenebutanol; 9-AP, 9-aminophenanthrene; ANF, α-naphthoflavone; 4PP, 4-phenylpyridine; 4-CPI, 4-(4-chlorophenyl)imidazole; TCEP, tris(2-carboxyethyl)phosphine; CYP or P450, cytochrome P450; EDTA, ethylenediaminetetraacetic acid; PMSF, phenylmethylsulfonylfluoride; ITC, isothermal titration calorimetry; ΔG, change in free energy; ΔH, change in enthalpy; ΔS, change in entropy; K_D, dissociation constant.

Acknowledgment. This work was supported in part by research grants from the Robert A. Welch foundation (H-1458) and NIH (GM54995) and by NIEHS Center Grant ES06676. Computational time was provided by the National Center for Supercomputing Applications (MCB050038N). We thank Christopher C. Chin for performing the analytical ultracentrifugation experiments and David Bolen for access to the VP−ITC instrument (Department of Biochemistry and Molecular Biology, UTMB). We thank Dmitri Davydov for the critical reading of this manuscript.

Supporting Information Available: Two figures and a table. Sedimentation velocity profiles of P450eryF, spectral titrations of competitive ligand binding with 1-PB and ANF, contact residues, and their distances from the docked ligands obtained from simulations. This material is available free of charge via the Internet at http://pubs.acs.org.

JA066303W